A Skeletally Diverse Library of Bioactive Natural Product-Like Compounds Enabled by Late-Stage P450-Catalyzed Oxyfunctionalization

Andrew R. Bortz[1,‡], John M. Bennett[1,‡], and Rudi Fasan[1,2]*

[1] *Department of Chemistry, University of Rochester; Rochester, NY, 14627, USA.*

[2] *Current affiliation: Department of Chemistry and Biochemistry, University of Texas at Dallas, 800 W. Campbell Road, Richardson, TX 75080, United States*

‡ These authors contributed equally to this work.

**Corresponding author. Email: rudi.fasan@utdallas.edu*

Keywords:

Diversity-oriented synthesis: chemoenzymatic synthesis; cytochrome P450 enzymes; C-H functionalization; chemical diversity; anticancer activity.

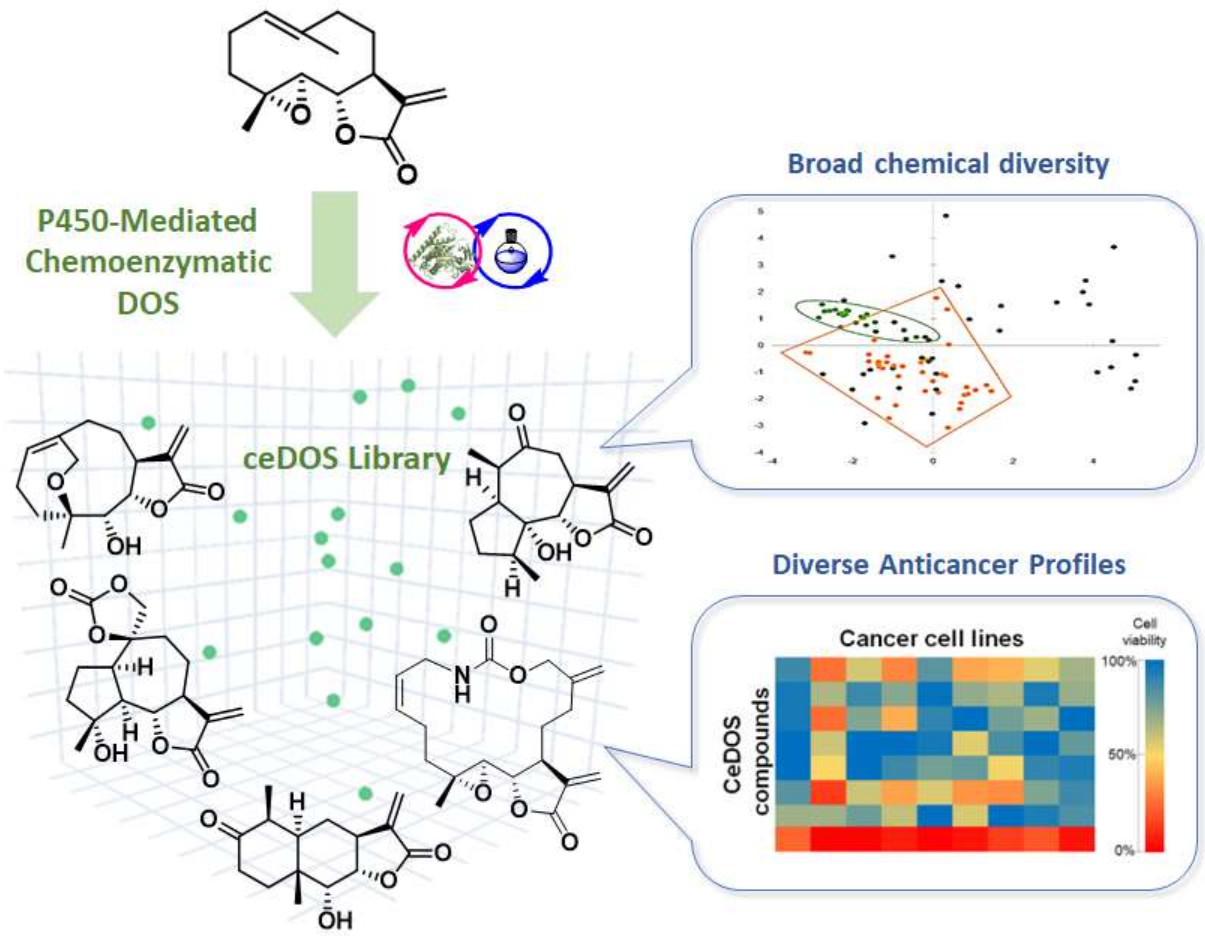

Highlights:

- New chemoenzymatic diversity-oriented strategy for synthesis of natural product-like molecules
- Chemo- and regiodivergent P450-catalyzed oxyfunctionalization as key step for skeletal diversification of parent scaffold
- Strategy enables access to unprecedented skeletons and enables the investigation of chemical space that map that of natural product based drugs.
- Discovered multiple library members exhibiting diversified anticancer activity profiles and cancer type selective cytotoxicity.

The Bigger Picture

Natural products and natural product-inspired molecules have constituted a major source of therapeutics and chemical agents for probing biological systems. We report the development of a new strategy for the synthesis of complex, natural product-like molecules that integrates regiodivergent, site-selective P450-catalyzed oxyfunctionalization with divergent chemical routes for skeletal diversification and rearrangement of a parent molecule. The resulting compound library, which comprises over 50 members equipped with an electrophilic warhead for covalent target protein engagement, is shown to encompass broad chemical and structural diversity and to include several bioactive compounds with selective cytotoxicity against cancer cells as well diversified anticancer activity profiles. This approach provides a new, powerful strategy for exploration of biologically relevant regions of the chemical space.

Summary

The discovery of small-molecule agents for chemical biology and therapeutic applications depends upon the ability to access and explore new biologically relevant regions of chemical space, a goal often pursued through diversity-oriented synthesis (DOS). In this report, we describe the design and implementation of P450-mediated chemoenzymatic diversity-oriented synthesis (CeDOS), a strategy that leverages chemo- and regiodivergent P450-catalyzed oxyfunctionalizations as key steps for enabling the synthesis of complex molecules that resemble natural products, a major source of bioactive molecules and drugs. Using this strategy, a library of over 50 novel and structurally diverse natural product-like compounds was generated through skeletal rearrangement and diversification of a plant-derived terpene via divergent chemoenzymatic routes enabled by selective C–H hydroxylation and epoxidation reactions catalyzed by engineered P450s. This CeDOS library encompass many unique and unprecedented organic scaffolds, many of which were determined to exhibit notable cytotoxicity against human cancer cells as well as diversified anticancer activity profiles. This work demonstrates the power of the present chemoenzymatic diversity-oriented synthesis strategy for directing the construction and discovery of novel bioactive molecules and it offers a blueprint for the broader application of this approach toward the creation and exploration of natural product-like chemical libraries.

Introduction

Natural products have provided a prominent source of therapeutic agents and small-molecule probes useful for perturbing and investigating cellular pathways [1, 2]. Structural complexity and skeletal diversity, along with a high content of stereogenic centers and sp^3 carbon atoms, are well known attributes that endow natural products with the ability to engage a variety of biological molecules with high affinity and specificity [3-6]. At the same time, these structural features make natural products challenging to synthesize and modify in an expeditious fashion [7-10]. While major advances in late-stage functionalization methods have enabled the synthesis of natural product analogs [11, 12], these approaches are inherently limited to the small fraction of natural products that can be harvested in relatively large quantities from natural sources. To overcome these challenges and because of the interest in enriching traditional combinatorial libraries with complex scaffolds [13-15], creative diversity-oriented synthesis (DOS) strategies have been developed to generate collections of small molecules that mimic the structural complexity and diversity of natural product scaffolds [16-23]. An early example is 'build/couple/pair' DOS [16, 24]. in which simple building blocks are coupled to make complex molecules in a few steps. Other notable approaches include the chemical diversification of natural product scaffolds [19-22] or natural product-inspired fragments [25, 26], biology-oriented synthesis [17, 27], and the assembly of stereochemically rich oligomers [28, 29]. Highlighting their importance, these DOS libraries have provided a source of bioactive compounds for chemical biology, as exemplified by the discovery of small-molecule modulators of the Sonic Hedgehog signaling pathway [30, 31], an inducer of ferroptosis [32], and GPCR inhibitors [33], among others. Despite this progress, DOS strategies have so far largely relied on the manipulation of functional groups preexisting (or pre-installed) in the parent scaffold/building blocks. In particular, methods for the site-selective functionalization of aliphatic C(sp^3)–H bonds, which are ubiquitous in organic molecules yet notoriously hard to target

with high selectivity, has remained largely untapped in DOS strategies useful for the construction of natural-product like compound libraries [34].

Among contemporary methods for late-stage C(sp^3)-H functionalization [11, 12], engineered cytochrome P450s have provided an attractive means to achieve this transformation through expansion of their substrate scope and manipulation of their regio- and stereoselectivity via protein engineering [35-39]. Leveraging this capability, engineered P450s have been exploited for the late-stage oxidation of complex molecules, including natural products, for further functional diversification by chemoenzymatic means (**Figure 1a**) [40-43]. More recently, selective C-H oxidation reactions catalyzed by natural or engineered P450s have been utilized for expediting the total synthesis of complex natural products (**Figure 1b**) [44-46]. In this work, we envisioned the opportunity to leverage P450-catalyzed site-selective C–H oxyfunctionalization as a key step for mediating the creation of natural product-like molecules via skeletal diversification of a parent scaffold by chemoenzymatic means (**Figure 1c**)**.** A key feature of this chemoenzymatic DOS strategy (CeDOS) is the exploitation of the enzymatically installed functional group (i.e., hydroxyl or epoxide) as a 'handle' for directing chemical rearrangement of the target scaffold in ways not attainable using the parent molecule or using purely chemical means. Here, we report the realization of this concept through the generation of a diverse collection of ~50 complex, natural product-like small molecules starting from plant-derived sequiterpene lactone parthenolide. As shown here, this approach can grant access to new *and* biologically relevant regions of chemical space, which overlaps with that of natural products and greatly extends beyond that accessible using late-stage C–H functionalization or total synthesis. In addition, this CeDOS library yielded several compounds that exhibit noticeable anticancer activity along with diversified anticancer

profiles, which showcases the power of this strategy toward enabling the discovery of novel bioactive molecules.

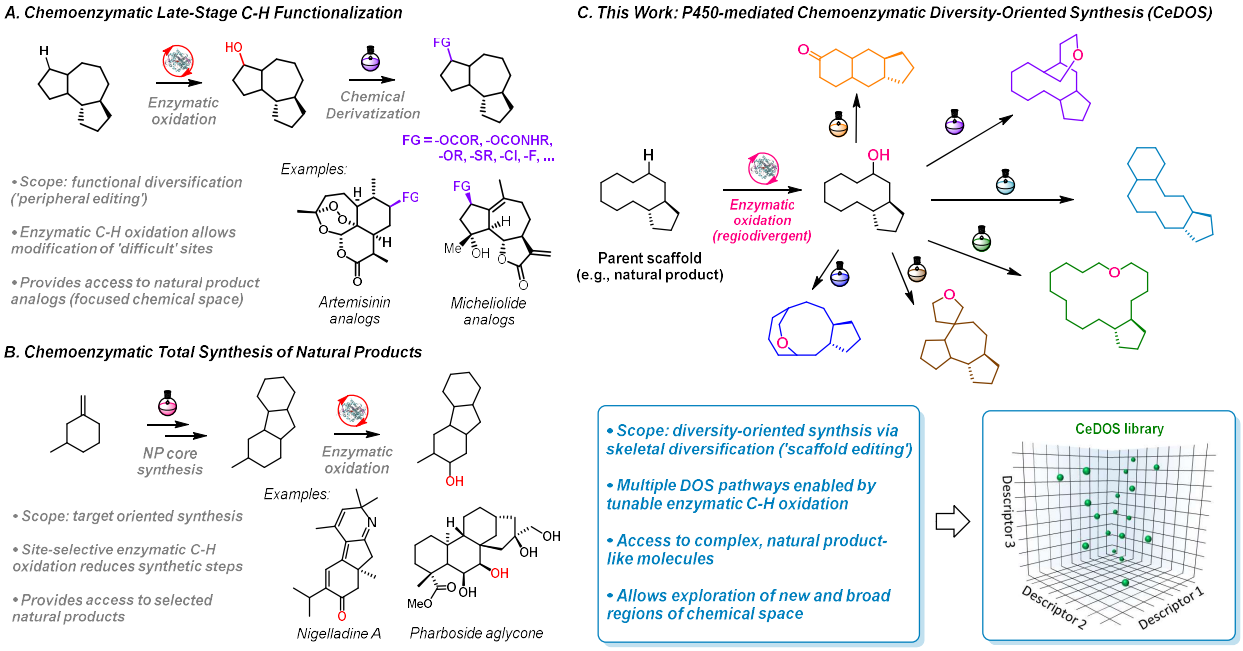

Figure 1. Natural product synthesis and diversification enabled by biocatalytic oxyfunctionalization. (**A**) Chemoenzymatic late-stage C–H functionalization of natural products for synthesis of natural product analogs. (**B**) Chemoenzymatic total syntheses of natural products through sequences incorporating cytochrome P450-catalyzed oxidations. (**C**) **This work**: Chemoenzymatic diversity-oriented synthesis (CeDOS) of a skeletally diverse library of natural product-like compounds enabled by site-selective P450-catalyzed oxyfunctionalization combined with divergent chemical routes.

Results and Discussion

To implement this strategy, we chose the sesquiterpene lactone parthenolide (PTL, **P01**) as a model target substrate by virtue of its prompt availability and its biological activity as an anticancer and anti-inflammatory agent [47, 48]. PTL's biological activity is linked to the presence of

an α-methylene-γ-lactone pharmacophore (**Figure 2**), which acts as electrophilic 'warhead' and mediates covalent engagement of its biological targets (e.g., NF-κB, IKK) via cysteine alkylation in these proteins [49, 50]. This reactive pharmacophore is also shared by other members of the sesquiterpene lactone family, which display diverse biological activities [51]. Because of that and the increasing interest in targeted covalent inhibitors [52, 53], we sought to implement our approach through the devise of chemoenzymatic routes that can allow for diversification of the PTL skeleton while leaving the α-methylene-γ-lactone warhead unaffected, since the latter was envisioned to confer biological activity in the resulting CeDOS compounds. Previous work in our group has developed engineered variants of the fatty acid hydroxylase $P450_{BM3}$ (*B. megaterium*) that can regio- and stereoselectively oxyfunctionalize PTL to give 9(*S*)-hydroxy-PTL (**P02**), 14-hydroxy-PTL (**P03**), and 1,10-epoxy PTL (**P04**), respectively (**Scheme S1**).[40] Briefly, a promiscuous $P450_{BM3}$ variant (FL#62) was initially identified that is able to oxidize PTL to give predominantly epoxide **P04** (77% select.) along with the hydroxylated PTL derivatives **P02** and **P03** as minor products (13% and 10% selectivity, respectively). The regioselectivity of this variant was then optimized by active site engineering in combination with P450 fingerprint[54] analysis, resulting in engineered P450 variants XII-F12 for selective production of **P02** (80% select; >99% *de*), XII-D8 for selective production of **P03** (95% select.), and III-D4 for selective production of **P04** (90% select.; >99% *de*) (**Scheme S1**).[40] According to our CeDOS strategy (**Figure 1C**), we envisioned these oxyfunctionalized products, which are unattainable by chemical means, could serve as critical intermediates for directing the skeletal rearrangement of PTL scaffold via divergent pathways.

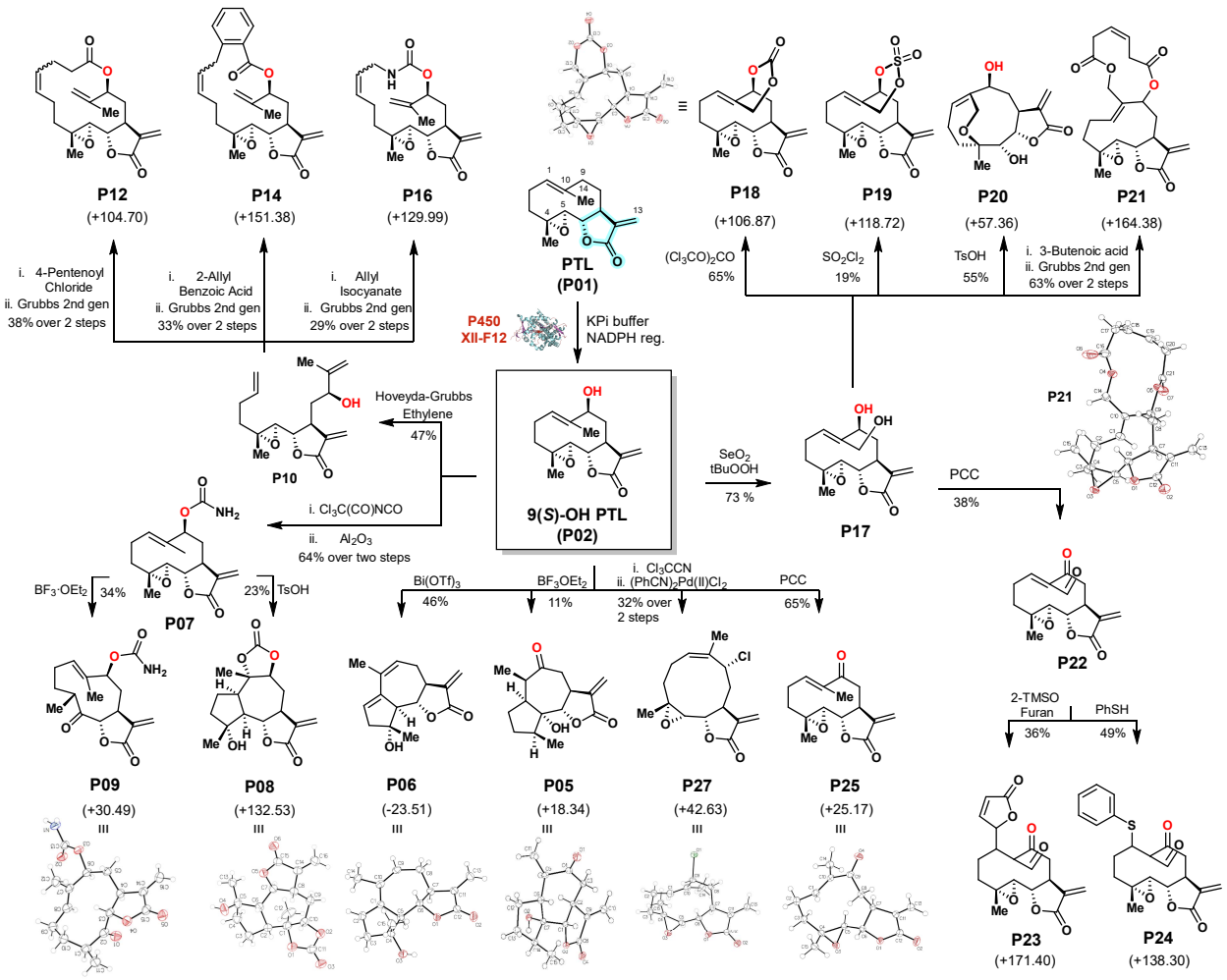

Figure 2. CeDOS compounds from chemoenzymatic diversification of 9(*S*)-hydroxy-parthenolide. Reaction conditions are provided in the supplementary material. In PTL, the α-methylene-γ-lactone moiety is highlighted in cyan. The values in parenthesis refer to difference in Böttcher complexity index scores (ΔC_m) between parthenolide and the CeDOS product. The structures of **P05**, **P06**, **P08**, **P09**, **P18**, **P21**, **P25**, and **P27** were determined by X-ray crystallographic analysis and are represented as ORTEP diagrams.

Skeletal diversification of PTL enabled by C9-hydroxylation

We began our studies by targeting 9(*S*)-hydroxy-PTL (**P02**) for structural diversification and leveraging the known ability of PTL to undergo structural rearrangements in the presence of Brønsted or Lewis acids [55]. Acid-catalyzed rearrangement of PTL is indeed known to produce the naturally occurring sesquiterpene lactone micheliolide (MCL) [56], a reaction that proceeds via a transannular cyclization resulting from intramolecular attack of the 1,10-olefin to the 4,5-epoxide ring activated by protonation (**Scheme S2**). This reaction is facilitated by the proximity of the olefin C1 to the C5 carbon of the epoxide ring and by the strain of the cyclodecene ring. Based on this knowledge, we envisioned that acid-catalyzed rearrangement of the hydroxylated PTL products **P02** (and **P03**) could afford new and interesting scaffolds via hijacking or redirecting this skeleton rearrangement pathway. Gratifyingly, two new 5,7-transannulated scaffolds **P05** and **P06** were obtained upon subjecting 9(*S*)-hydroxy-PTL to Lewis acidic conditions in the presence of boron trifluoride (BF_3) or bismuth triflate ($Bi(OTf)_3$), respectively (**Figure 2**). Both of these products feature a tricyclic skeleton similar to that shared by bioactive members of guaian-6,12-olide family of natural products (**Figure S1**) [57]. We further hypothesized that a nucleophilic group appended to the C9 hydroxyl group might redirect the acid-induced rearrangement pathway by intercepting the transient carbocation species formed in the acid-induced PTL→MCL rearrangement (**Scheme S2**), affording new scaffolds. To this end, we prepared carbamate **P07** using a mild two-step carbamoylation/hydrolysis sequence. Gratifyingly, exposure of **P07** to Brønsted acidic conditions (TsOH) promoted cyclization of the carbamate to yield **P08**, which contains a cyclic carbonate motif—rarely found in natural products—fused to a guaianolide-type cycloheptane ring. We propose this product is formed by acid-catalyzed transannular cyclization, followed by trapping of the carbocation intermediate by the carbamate group, and subsequent

hydrolysis of the ensuing dioxolanimine (**Scheme S3**). Interestingly, treatment of carbamate **P07** with Lewis acid BF_3 gave instead the Meinwald-like rearrangement product **P09**, which features an altered carbocyclic scaffold compared to PTL as revealed by X-ray crystallography (**Figure 2**). Of note, treatment of PTL under these conditions produces only MCL, highlighting the ability of the (chemo)enzymatically installed functional group to reprogram the outcome of the scaffold rearrangement reaction, as observed for the other products discussed earlier. In the case of **P09**, the carbamate group likely restricts rotation of the backbone scaffold making rearrangement of the 4,5-epoxide more favorable than the transannular cyclization pathway leading to MCL.

We next targeted the internal 1,10-olefin for further PTL skeletal diversification. In their work toward the total synthesis of PTL, Arndt and coworkers noted the challenges associated with the final macrocyclization via ring-closing metathesis (RCM), observing optimal cyclization in the presence of two terminal olefins [58]. These results suggested to us that a ring-opening metathesis process may instead be favorable, with the resulting ring-opened product being unreactive towards RCM. In turn, we envisioned this would provide an opportunity to access new complex scaffolds via a telescoped RCM. Following this plan, 9(*S*)-hydroxy-PTL could be readily converted to the linear, ring-opened product **P10** by employing Hoveyda-Grubbs II catalyst in the presence of ethylene (**Figure 2**). A terminal olefin was then appended to the enzymatically installed C9 hydroxyl group to set the stage for macrocyclization via RCM. To our delight, esterification of **P10** with 4-pentenoyl chloride and subsequent RCM delivered macrocycle **P12**. Further highlighting the modularity of this CeDOS route, **P10** was leveraged as key intermediate to access macrocycles **P14** and **P16**, which differ from each other and **P12** by the nature of the tether and functionalities embedded in the ring. While unprecedented, these compounds feature molecular

skeletons reminiscent of those found in various bioactive polyketides or other macrocyclic natural products such as cembranolides, which includes the antimicrobial agent ovatodiolide (**Figure S1**).

Oxidation of PTL with selenium dioxide (SeO_2) is known to result in the allylic oxidation of the C14 methyl group albeit with concurrent *E*→*Z* isomerization of the 10,11 double bond to give melampomagnolide B.[59] Based on this knowledge, we hypothesized that oxidation of 9(*S*)-hydroxy-PTL under similar conditions could furnish a diol intermediate useful for building further structural complexity. Accordingly, treatment of 9(*S*)-hydroxy-PTL with SeO_2 in the presence of *tert*-butyl hydroperoxide afforded diol **P17**. In stark contrast to PTL, however, allylic oxidation of C14 in 9(*S*)-hydroxy-PTL was not accompanied by isomerization of the 1,10 double bond, further highlighting the impact of enzymatic oxidation on the reactivity of the parent scaffold. Importantly, the spatial proximity of the two hydroxy groups at C9 and C14 in **P17**, along with the preserved *trans* configuration of the 1,10 double bond, set the stage for the following scaffold rearrangement reactions. Indeed, treatment of **P17** with either triphosgene or sulfuryl chloride allowed bridging of the diol to afford the polycyclic compounds **P18** and **P19**, respectively. Based on our results with **P08**, we further envisioned that either of the hydroxy group in **P17** might be able to hijack the acid-catalyzed ring rearrangement pathway mentioned earlier. Interestingly, treatment of **P17** with pTsOH afforded the unique ether-bridged scaffold **P20**. As for **P28** (*vide infra*), we propose this reaction involves a direct nucleophilic attack of the C14 hydroxyl group to the acid-activated 4,5-epoxide (**Scheme S4**), thus offering another unique mode of intramolecular cyclization useful for PTL skeletal diversification. Again, the reactivity of these compounds override the inherent propensity of PTL to give a MCL-like scaffold under acidic conditions, further highlighting the critical role of P450-mediated oxidation in influencing the outcome of the skeletal rearrangement reaction. To our knowledge, the biocyclo[5.3.2] architecture of **P20** and **P28** is unprecedented

among natural and synthetic molecules alike. Lastly, diesterification of diol **P17** to introduce two pendant terminal olefin groups, followed by RCM afforded the 10,11-fused-bicyclic macrolide-like compound **P21**.

The enzymatic oxidation site in **P17** was further exploited to activate the 1,10-double bond for structural diversification via 1,4-additions. To this end, **P17** was oxidized to 1,3-dicarbonyl compound **P22**, in which C1 position is strongly primed for attack by soft nucleophiles (over the electrophilic C13 site). Treatment of **P22** with either 2-(trimethylsiloxy)furan (TMSOF) or thiophenol afforded the new scaffolds **P23** and **P24**, respectively. **P23** is reminiscent of the antimicrobial mikanolide from *M. micrantha* (**Figure S1**), both incorporating a butanolide moiety as second electrophilic warhead. Similarly to **P23**, oxidation of 9(*S*)-hydroxy parthenolide yielded **P25**, which also contains a dual electrophilic warhead. As revealed by its crystal structure, this subtle structural modification ($CH_2 \rightarrow CO$) induces a major twist of the carbocyclic scaffold in **P25** compared to PTL, resulting from flipping of the spatial orientation of both the 1,10 olefin and C14 methyl group (**Figure 2**). Lastly, we envisioned a potential 2,3-sigmatropic rearrangement through the trichloroacetimidate derivative **P26 (Scheme S5)**. Instead of the sigmatropic rearrangement product, treatment of **P26** under Overman rearrangement conditions afforded **P27**, which exhibits another unique scaffold as a result of 1,10-double bond isomerization and chlorination of position C9 (**Figure 2**).

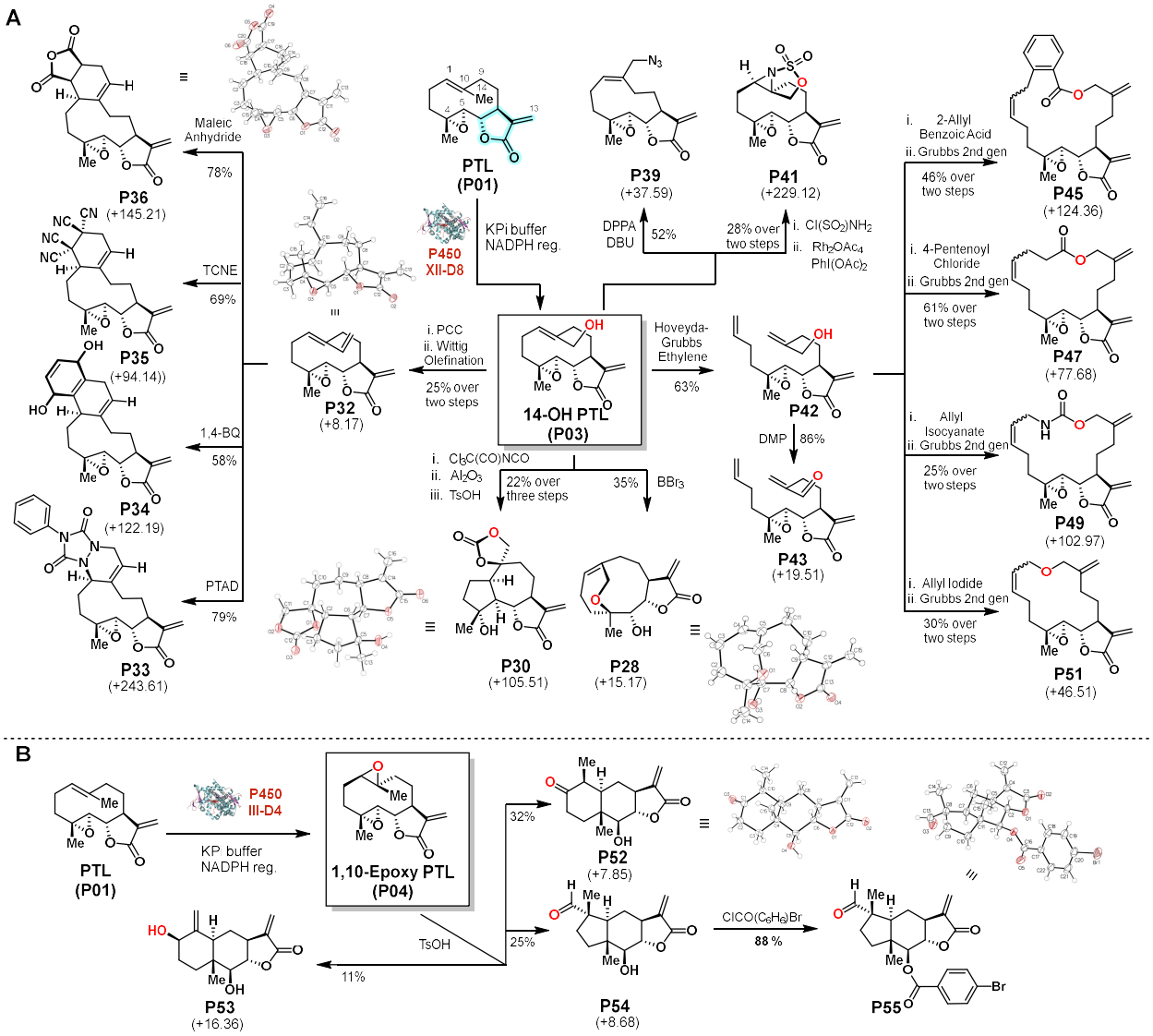

Figure 3. Diverse CeDOS compounds from chemoenzymatic diversification of (A) 14-hydroxy-PTL and (B) 1,10-epoxy parthenolide. Reaction conditions are provided in the supplementary material. Isolated yields are reported along with the difference in Böttcher complexity index scores (ΔC_m) between parthenolide and the CeDOS product. The structures of P28, P30, P32, P36, P52 and P55 were determined by x-ray crystallographic analysis and are represented as ORTEP diagrams.

Skeletal diversification of PTL enabled by C14-hydroxylation and 1,10-epoxidation.

Next, we turned our attention to the skeletal rearrangement of 14-hydroxy-PTL (**P03, Figure 3A**), which is uniquely accessible via the present enzymatic strategy due to propensity of PTL to undergo 1,10 double bond isomerization upon allylic oxidation of the C14 position via chemical means as noted above.[59] Based on the results with **P20**, treatment of 14-hydroxy-PTL with boron tribromide (BBr_3) resulted in a similar acid-catalyzed rearrangement with trapping of the carbocation intermediate by the enzymatically installed alcohol group to afford **P28**, which exhibits a rather unique molecular architecture as revealed by crystallography (**Figure 3A**). We further speculated that carbamoylation of the 14-hydroxy group could either provide an alternative nucleophile for epoxide ring opening (as in **P28**) or disable this mode of rearrangement and capture the transient carbocation species resulting from transannular cyclization (as in **P08**). Interestingly, acid (pTsOH)-induced rearrangement of carbamate **P29** (**Scheme S6**) favored the carbocation trapping product to yield the spirocyclic carbonate scaffold **P30** (**Figure 3A**).

DOS strategies often rely on transformations that can rapidly diversify a common precursor via a set of different reagents [60, 61]. Amongst these, Diels-Alder [4+2] cycloadditions are often employed during the final "pairing" step in so-called 'build-couple-pair' DOS strategies [29]. Inspired by these examples, **P03** was converted to 1,3-diene **P32** via oxidation of the C14 hydroxyl group, followed by Wittig olefination. To our delight, reaction of **P32** with 4-phenyl-1,2,4-triazoline-3,5-dione (PTAD) afforded the desired cycloaddition product **P33** as a single diastereomer. Furthermore, this strategy could be readily extended to other dienophiles to afford **P34, P35**, and **P36**, which incorporate varying degrees of ring, functionality, and stereochemical complexity onto the cyclodecene scaffold (**Figure 3A**). The absolute configuration of the C1 stereocenter in these molecules was determined by NOESY experiments (**P33**) and X-ray

crystallography (**P36**) and its *R* configuration, along with absolute diastereoselectivity of these cycloaddition reactions, can be rationalized based on the geometric constraints of Diels-Alder cycloaddition reactions and the steric accessibility to attack by the dienophile of only the *re* face of the 1,10-double bond in **P32**, as evinced from its crystal structure (**Figure 3**).

Notably, 9(*S*)-hydroxy-PTL (**P02**) could be also converted to 1,3-diene **P37** via a similar oxidation/aldehyde olefination sequence as applied to prepare **P32**. However, in contrast to the latter, **P37** showed no reactivity toward most dienophiles, while reaction with PTAD exclusively produced the disubstituted scaffold **P38** (**Scheme S7**). The differential reactivity of the **P02**- vs. **P03**-derived diene in these reactions further highlight the benefits of tunable site-selectivity offered by P450-catalyzed C-H oxidation step for the purpose of skeletal diversification.

Following an alternate CeDOS trajectory, we explored different intramolecular cyclization chemistries for targeting either the 1,10-olefin or adjacent allylic C-H bond via a pendant group installed at C14. Among them, intramolecular aziridination proved fruitful, enabling the synthesis of **P41** from sulfamate intermediate **P40** via a rhodium-catalyzed intramolecular nitrene insertion reaction in the presence of hypervalent iodine reagent (**Scheme S8**). This reaction creates two new stereogenic centers in a highly stereoselective fashion, producing a complex polycyclic scaffold. **P41** features a sulfamate moiety, which is scarce in natural products but common in drug molecules [62], along with a tertiary aziridine ring, a reactive moiety found in various bioactive natural products [63].

To further expand our CeDOS library, we capitalized on the ring opening/closing metathesis strategy developed for diversification of 9(*S*)-hydroxy-PTL (**Figure 2**). Accordingly, 14-hydroxy-PTL could be efficiently converted to **P42** via ring-opening metathesis. After appending a terminal olefin to the enzymatically installed C14 alcohol group through different

tethers, ring-closing metathesis furnished access to macrocycles **P45**, **P47** and **P49** (**Figure 3A**). Because of the different site of enzymatic C-H hydroxylation used for tethering, these compounds feature different macrocycle size (i.e., 16-17 vs. 14-15 membered rings) and stereochemical complexity compared to the RCM products derived from 9(*S*)-hydroxy-PTL (**P12, P14, P16; Figure 2**). In addition, leveraging the reduced steric hindrance of the primary alcohol in **P42** (vs. secondary alcohol in **P10**), the ether-linked macrocycle **P51** could be also obtained upon alkylation of **P42** with allyl iodide, followed by macrocyclization via RCM. It is worth noting that while **P10**, **P42**, and **P43** served as versatile intermediates for the RCM-mediated macrocyclizations, their structures resemble those of a variety of 'linear' bioactive sesquiterpene lactones found in plants (e.g. anthecotuloide; **Figure S1**). Following yet another CeDOS path, and based on the known propensity of allylic azides to undergo Winstein rearrangements [64], we targeted the rearrangement of 14-azido-PTL, which was accessed via azidation of 14-hydroxy-PTL. Interestingly, reaction of **P03** with diphenylphosphorylazide (DPPA) provided efficient access to the Z-configured azido derivative **P39** (**Figure 3**), in which isomerization of the 1,10 double bond likely occurs as a result of an ionic azidation mechanism, and/or a double Winstein rearrangement, driven by ring strain release. The azido group in **P39** provides a versatile handle for further elaboration of this molecule via azide/alkyne cycloaddition reactions.

Lastly, we targeted the diversification of the enzymatic product 1(*R*),10(*R*)-epoxy-PTL (**P04**, **Figure 3B**). In this compound, an epoxide replaces the 1,10-olefin responsible for the acid-mediated transannular cyclization pathway that normally drive the conversion of PTL to MCL (**Figure S2**). Because this pathway is disabled in **P04**, we envisioned this compound could exhibit unique reactivity *vis-à-vis* with PTL under acidic conditions. Indeed, exposure of **P04** to tosylic acid resulted in major structural rearrangement of the molecule to afford products **P52, P53**, and

P54 (**Figure 3B**). While never described before, **P52** and **P53** share the tricyclic scaffold found in eudesmanolide-type natural products (**Figure S1**), which have been reported to possess anti-cancer and anti-viral activities [65]. On the other hand, **P54** features an entirely novel skeleton compared to known synthetic or natural compounds. Altogether, these results showcase the capability of the present CeDOS strategy to provide access to a unique and diverse range of structurally complex molecular scaffolds (51 in total). Furthermore, as illustrated with the synthesis of **P55**, most of these compounds incorporate functional groups useful for further derivatization/diversification.

Analysis of chemical diversity of CeDOS library

Whereas crystallographic analysis of representative CeDOS compounds provide insights into their structural diversity (**Figures 2** and **3**), we sought to assess the diversity encompassed by the compound collection in a more systematic manner using chemoinformatic tools. To this end, the Böttcher score (C_m), an additive measure of molecular complexity [66], was calculated for each compound and compared to PTL (**Table S1**). All members of the CeDOS library, except one (**P06**), showed a greater molecular complexity than PTL (ΔC_m range: +8 to +244), with the maximum and average complexity index of the library being ~83% and ~29% greater than PTL's, respectively. These parameters indicate that a significant degree of molecular complexity is added to the parent molecule through the CeDOS transformations. To further assess the diversity of the library, the structural similarity between each compound vs PTL and any other member of the collection was measured using the Tanimoto coefficient [67]. As illustrated by the matrix in **Figure 4A** (see complete data in **Figure S1**), this analysis indicated a significant degree of structural diversity across the CeDOS collection, with most dissimilar compounds featuring Tanimoto coefficient as low as 0.45-0.50. As expected, compounds generated via similar CeDOS strategies

show greater degrees of similarity with one another vs. other members of the library (e.g. **P34-P36** or **P52-P54**). The chemical diversity encompassed by the CeDOS library was also analyzed via principal component analysis (PCA) [68] using a set of 13 different physicochemical descriptors, including H-bond donor/acceptor density, LogP, rotatable bonds, and ring/stereochemical complexity (**Figure 4B**). For comparison, the same analysis was conducted on (a) a diverse panel of 42 FDA-approved natural product-derived drugs, and (b) a panel of parthenolide analogs we previously generated via chemoenzymatic late-stage C–H functionalization (**Figure S3**) [40, 69]. As shown in **Figure 4B**, this analysis showed that, similar to the NP drug library, the CeDOS library encompasses a wide region of chemical space, which is particularly remarkable considering that the entire collection was derived from a single parent molecule (**Figure 4B**). In addition, the CeDOS library encompasses both a distinct and significantly larger area of the chemical space when compared to that covered by PTL analogs obtained by 'peripheral editing' through late-stage C–H functionalization (**Figure 1A**), which highlights both the complementarity of two strategies and the advantage of the present method toward generating new chemical diversity.

We further analyzed selected physiochemical properties of the CeDOS compounds that are relevant for medicinal chemistry (e.g., *n*-octanol/water partition coefficient (ClogP), number of stereocenters, and fraction of sp^3-hybridized carbons (Fsp^3)). As shown in **Figure 4C**, 95% of the CeDOS compounds possess a CLogP value between 1 and 3 (avg: 2.20), which falls within the optimal range (ClogP: 0-3) for good oral and intestinal absorption. High degrees of chirality and three-dimensionality (estimated by their Fsp^3 values) are highly sought after in small-molecule libraries for drug discovery as these features are typically associated with higher target specificity and lower potential for off-target effects compared to achiral and 'flat' (sp^2-rich) molecules [3-6]. Reflecting its high degrees of three-dimensionality and stereochemical richness, the average

number of stereocenters of the CeDOS library is >20-fold greater than that of a traditional combinatorial chemistry library (5.05 vs. 0.24), whereas its average Fsp^3 value is nearly threefold higher (0.60 vs. 0.23). In addition, nearly all of the CeDOS library members satisfy criteria associated with favorable drug pharmacokinetics [70] (**Figure S4**). Altogether, these data support the effectiveness of the present approach toward generating structurally diverse compounds that also possess desirable drug-like properties.

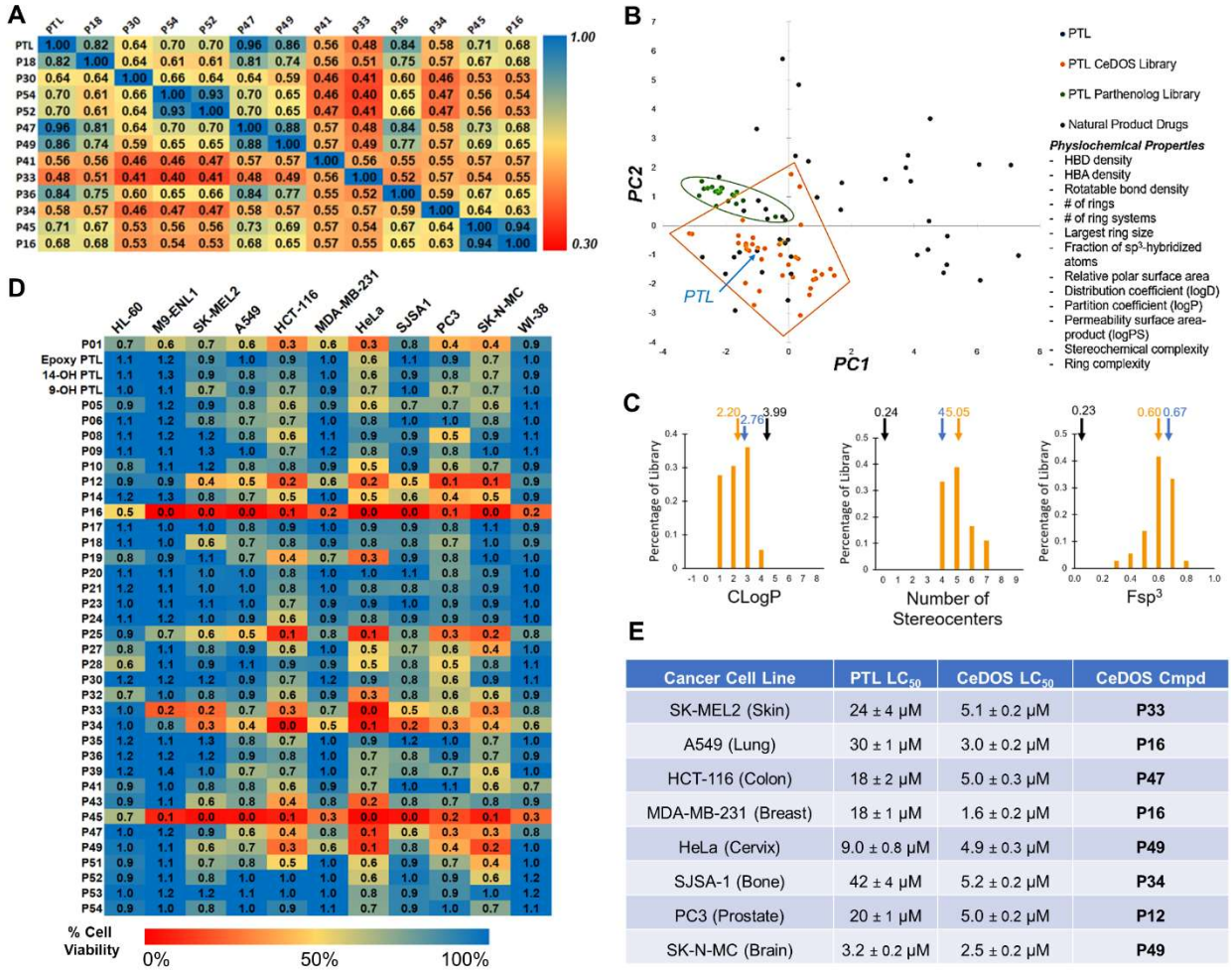

Cancer Cell Line	PTL LC_{50}	CeDOS LC_{50}	CeDOS Cmpd
SK-MEL2 (Skin)	24 ± 4 μM	5.1 ± 0.2 μM	**P33**
A549 (Lung)	30 ± 1 μM	3.0 ± 0.2 μM	**P16**
HCT-116 (Colon)	18 ± 2 μM	5.0 ± 0.3 μM	**P47**
MDA-MB-231 (Breast)	18 ± 1 μM	1.6 ± 0.2 μM	**P16**
HeLa (Cervix)	9.0 ± 0.8 μM	4.9 ± 0.3 μM	**P49**
SJSA-1 (Bone)	42 ± 4 μM	5.2 ± 0.2 μM	**P34**
PC3 (Prostate)	20 ± 1 μM	5.0 ± 0.2 μM	**P12**
SK-N-MC (Brain)	3.2 ± 0.2 μM	2.5 ± 0.2 μM	**P49**

Figure 4. Chemical diversity and anticancer activity of CeDOS library. A) Tanimoto similarity matrix of select CeDOS compounds. See **Figure S2** for complete data. **B**) Principal

component analysis (PCA) of the physiochemical properties of CeDOS library (orange) vs. collection of FDA-approved natural product based drugs (42 compounds, grey; **Table S2**) and a library of PTL analogs obtained via late-stage C–H functionalization [40, 69] (20 compounds, green; **Figure S3**). The parent molecule (PTL, blue) is indicated. **C**) Histograms of the ClogP values, number of stereocenters, and fraction of sp^3-hybridized carbon atoms (F_{sp}^3) of the CeDOS library, with arrows indicating the average values for the CeDOS library (orange), PTL (blue), and the average value for a commercial library (ChemBridge MicroFormat Library [20], black). **D**) Heatmap representing the cytotoxicity of the CeDOS library against a panel of eight cancer cell lines and a non-cancerous cell line (WI-38) as determined via single-dose cell viability assay (10 μM compound, 24 hrs). See **Figure S5** for additional data. **E)** Half-maximal lethal concentration (LC_{50}) values for PTL and select compounds from the CeDOS library. LC_{50} values are reported as mean ± SD (n = 3). See **Table S3** for additional data.

Anticancer activity of CeDOS compounds

As proof-of-principle assessment of the biological activity of the CeDOS library, the compounds were tested for cytotoxicity against a diverse panel of human cancer cell lines, encompassing both solid (skin, lung, colon breast, cervical, bone, prostate, brain) and hematologic tumors (leukemia, lymphoma). As illustrated by the cell viability data in **Figures 4D** and **S5**, the CeDOS compounds were found to exhibit a diverse range of anticancer activity profiles, including compounds with broad-spectrum cytotoxicity (i.e., **P16, P45**) as well as compounds with both intermediate (e.g., **P12, P25, P33, P34)** and high cancer-type specificity (e.g., **P19**, **P32**, **P43**). Whereas several members of the library showed significantly enhanced cytotoxicity compared to

PTL and its oxyfunctionalized derivatives (**P2-P5**), most of the active compounds, with the only exception of broad-spectrum ones, also showed little to no toxicity against normal cells (WI-38, lung fibroblast; **Figure 4D**), demonstrating that their activity is specific against cancer cells. The lack of activity of certain members of the library (e.g., **P17**, **P53**) further showed that the α-methylene-γ-lactone warhead is not sufficient for anticancer activity, indicating that the rest of the scaffold largely dictates activity and cancer cell specificity. Other notable structure-activity insights include the large impact on the linkage utilized for macrocyclization of 14-hydroxy-PTL-derived **P45** and **P49** on the cancer cell specificity of these molecules. Similarly, the cyclic sulfate vs. cyclic carbonate ring in **P19** vs. **P18** confers the former with selective activity against colon (HCT-116) and cervical (HeLa) cancer cells, while **P18** displays little anticancer activity. Lastly, the Diels-Alder cycloaddition products **P33** and **P34** motifs showed noticeable anticancer activity against six or more cell lines (<10% cell viability at 10 μM), whereas the alternate cycloaddition products **P35** and **P36** show modest to no activity against the same cell lines (**Figure 4D**), further highlighting the impact of the CeDOS diversification strategies on the anticancer profile of these compounds. Importantly, as determined based on their half-maximal lethal dose (LD_{50}) values (**Figure 4E**), for each of the cancer cell lines at least one member of the CeDOS library was found to possess markedly enhanced anticancer potency compared to PTL. These include **P16**, which show ≥10-fold enhanced potency against lung adenocarcinoma (A549) and breast cancer cells (MDA-MB-231), and compound **P47**, with >3-fold increased potency against colon cancer cells (HCT-116). Altogether, these results demonstrate the effectiveness of the present CeDOS in delivering bioactive compounds with selective cytotoxicity against cancer cells as well as diversified anticancer activity profiles.

Conclusion

In summary, we have developed a new chemoenzymatic DOS strategy that integrates enzymatic late-stage oxidation with divergent, chemical transformations to produce a diverse collection of complex molecules. As shown here, chemo- and regiodivergent P450-catalyzed oxidations are leveraged as key points of entry for permitting a series of diversity-generating transformations that would be otherwise inaccessible, or not readily attainable, in the parent molecule. Using this strategy, it became possible to generate a collection of >50 novel natural product-like compounds that display high structural and stereochemical complexity as well as large degrees of diversity in terms of physiochemical properties and biological activity. Notably, many of these compounds were found to exhibit potent anticancer activity as well as diversified cancer cell specificity profiles, which highlights the value of this method for the discovery of small molecules with relevant biological activity. Given the ability of natural or engineered P450s to hydroxylate a variety of complex natural products and drugs [36-46, 71-76], we envision that this CeDOS strategy can be extended to other natural or synthetic complex molecules as starting points for library generation via P450-mediated chemoenzymatic scaffold diversification, in order to unlock other unique and currently unexplored and/or inaccessible molecular skeletons. As demonstrated in the case of PTL [40] and other complex terpene natural products [37, 42], P450 fingerprint based strategies can be applied to guide protein engineering of these enzymes and obtain variants with fine-tuned regio- and stereoselectivity for preparative scale synthesis. Alternatively, P450 library screening [36, 43, 72, 76] or rational design [38, 39, 75] have been successfully applied to generate variants with improved regio- and stereoselectivity toward a substrate of interest. We also anticipate that this approach can be integrated with other enzymatic systems useful for selective C-H

functionalization, including through new-to-nature chemistries[77, 78], as a powerful means to expand opportunities for the discovery of new bioactive molecules for medicine and chemical biology.

AUTHOR INFORMATION

Corresponding Authors:

* rudi.fasan@utdallas.edu.

ACKNOWLEDGMENTS

This work was supported by the U.S. National Institute of Health grant GM098628 (R.F.). R.F. acknowledges support from the Cancer Prevention and Research Institute of Texas (CPRIT RR230018) and Robert A. Welch Foundation (Chair, AT-0051). J. M. B. is a trainee in the Medical Scientist Training Program funded by NIH T32 GM007356. The authors are grateful to Dr. William Brennessel and Dr. Harry Stern (University of Rochester) for assistance with crystallographic analyses and Tanimoto analyses, respectively. MS and X-ray instrumentation at the University of Rochester are supported by U.S. National Science Foundation grants CHE-0946653 and CHE-1725028 and the U.S. National Institute of Health grant S10OD030302. This work is dedicated to the memory of Prof. Robert K. Boeckman, Jr..

Author contributions

A.R.B. and R.F. conceived the project; A.R.B. and J.M.B. designed and executed the experiments, with input and guidance from R.F.; J.M.B. performed the chemoinformatic analyses and biological testing. All authors discussed the results and wrote the manuscript.

Data and materials availability

All data are available in the main text or the supplementary information.

References

(1) Butler, M. S. Natural products to drugs: natural product-derived compounds in clinical trials, *Nat. Prod. Rep.* **2008**, *25*, 475-516.

(2) Cragg, G. M., Grothaus, P. G., and Newman, D. J. Impact of natural products on developing new anti-cancer agents, *Chem. Rev.* **2009**, *109*, 3012-3043.

(3) Clemons, P. A., Wilson, J. A., Dancik, V., Muller, S., Carrinski, H. A., Wagner, B. K., Koehler, A. N., and Schreiber, S. L. Quantifying structure and performance diversity for sets of small molecules comprising small-molecule screening collections, *Proc. Natl. Acad. Sci. U. S. A.* **2011**, *108*, 6817-6822.

(4) Feher, M., and Schmidt, J. M. Property distributions: differences between drugs, natural products, and molecules from combinatorial chemistry, *J. Chem. Inf. Comput. Sci.* **2003**, *43*, 218-227.

(5) Tan, D. S. Diversity-oriented synthesis: exploring the intersections between chemistry and biology, *Nat. Chem. Biol.* **2005**, *1*, 74-84.

(6) Welsch, M. E., Snyder, S. A., and Stockwell, B. R. Privileged scaffolds for library design and drug discovery, *Curr. Opin. Chem. Biol.* **2010**, *14*, 347-361.

(7) Young, I. S., and Baran, P. S. Protecting-group-free synthesis as an opportunity for invention, *Nat. Chem.* **2009**, *1*, 193-205.

(8) Wu, Z. C., and Boger, D. L. The quest for supernatural products: the impact of total synthesis in complex natural products medicinal chemistry, *Nat. Prod. Rep.* **2020**.

(9) Truax, N. J., and Romo, D. Bridging the gap between natural product synthesis and drug discovery, *Nat. Prod. Rep.* **2020**, *37*, 1436-1453.

(10) Lia, J., Amatuni, A., and Renata, H. Recent advances in the chemoenzymatic synthesis of bioactive natural products, *Curr. Opin. Chem. Biol.* **2020**, *55*, 111-118.

(11) Guillemard, L., Kaplaneris, N., Ackermann, L., and Johansson, M. J. Late-stage C-H functionalization offers new opportunities in drug discovery, *Nat. Rev. Chem.* **2021**, *5*, 522-545.

(12) Hong, B. K., Luo, T. P., and Lei, X. G. Late-Stage Diversification of Natural Products, *ACS Cent. Sci.* **2020**, *6*, 622-635.

(13) Lachance, H., Wetzel, S., Kumar, K., and Waldmann, H. Charting, Navigating, and Populating Natural Product Chemical Space for Drug Discovery, *J. Med. Chem.* **2012**, *55*, 5989-6001.

(14) Kodadek, T. The rise, fall and reinvention of combinatorial chemistry, *Chemical Communications* **2011**, *47*, 9757-9763.

(15) Lovering, F., Bikker, J., and Humblet, C. Escape from Flatland: Increasing Saturation as an Approach to Improving Clinical Success, *Journal of Medicinal Chemistry* **2009**, *52*, 6752-6756.

(16) Burke, M. D., Berger, E. M., and Schreiber, S. L. Generating diverse skeletons of small molecules combinatorially, *Science* **2003**, *302*, 613-618.

(17) Wetzel, S., Bon, R. S., Kumar, K., and Waldmann, H. Biology-Oriented Synthesis, *Angew. Chem. Int. Ed.* **2011**, *50*, 10800-10826.

(18) Wender, P. A., Verma, V. A., Paxton, T. J., and Pillow, T. H. Function-oriented synthesis, step economy, and drug design, *Acc. Chem. Res.* **2008**, *41*, 40-49.

(19) Balthaser, B. R., Maloney, M. C., Beeler, A. B., Porco, J. A., and Snyder, J. K. Remodelling of the natural product fumagillol employing a reaction discovery approach, *Nat. Chem.* **2011**, *3*, 969-973.

(20) Huigens, R. W., Morrison, K. C., Hicklin, R. W., Flood, T. A., Richter, M. F., and Hergenrother, P. J. A ring-distortion strategy to construct stereochemically complex and structurally diverse compounds from natural products, *Nat. Chem.* **2013**, *5*, 195-202.

(21) Rafferty, R. J., Hicklin, R. W., Maloof, K. A., and Hergenrother, P. J. Synthesis of Complex and Diverse Compounds through Ring Distortion of Abietic Acid, *Angew. Chem. Int. Ed.* **2014**, *53*, 220-224.

(22) Paciaroni, N. G., Ratnayake, R., Matthews, J. H., Norwood, V. M., Arnold, A. C., Dang, L. H., Luesch, H., and Huigens, R. W. A Tryptoline Ring-Distortion Strategy Leads to Complex and Diverse Biologically Active Molecules from the Indole Alkaloid Yohimbine, *Chem. Eur. J.* **2017**, *23*, 4327-4335.

(23) Gerlach, E. M., Korkmaz, M. A., Pavlinov, I., Gao, Q. W., and Aldrich, L. N. Systematic Diversity-Oriented Synthesis of Reduced Flavones from gamma-Pyrones to Probe Biological Performance Diversity, *ACS Chem. Biol.* **2019**, *14*, 1536-1545.

(24) Burke, M. D., and Schreiber, S. L. A planning strategy for diversity-oriented synthesis, *Angew. Chem. Int. Ed.* **2004**, *43*, 46-58.

(25) Kim, J., Kim, H., and Park, S. B. Privileged Structures: Efficient Chemical "Navigators" toward Unexplored Biologically Relevant Chemical Spaces, *J. Am. Chem. Soc.* **2014**, *136*, 14629-14638.

(26) Kopp, F., Stratton, C. F., Akella, L. B., and Tan, D. S. A diversity-oriented synthesis approach to macrocycles via oxidative ring expansion, *Nat. Chem. Biol.* **2012**, *8*, 358-365.

(27) Karageorgis, G., Foley, D. J., Laraia, L., and Waldmann, H. Principle and design of pseudo-natural products, *Nat. Chem.* **2020**, *12*, 227-235.

(28) Aquino, C., Sarkar, M., Chalmers, M. J., Mendes, K., Kodadek, T., and Micalizio, G. C. A biomimetic polyketide-inspired approach to small-molecule ligand discovery, *Nat. Chem.* **2012**, *4*, 99-104.

(29) Spiegel, D. A., Schroeder, F. C., Duvall, J. R., and Schreiber, S. L. An oligomer-based approach to skeletal diversity in small-molecule synthesis, *J. Am. Chem. Soc.* **2006**, *128*, 14766-14767.

(30) Stanton, B. Z., Peng, L. F., Maloof, N., Nakai, K., Wang, X., Duffner, J. L., Taveras, K. M., Hyman, J. M., Lee, S. W., Koehler, A. N., Chen, J. K., Fox, J. L., Mandinova, A., and Schreiber, S. L. A small molecule that binds Hedgehog and blocks its signaling in human cells, *Nat. Chem. Biol.* **2009**, *5*, 154-156.

(31) Kremer, L., Hennes, E., Brause, A., Ursu, A., Robke, L., Matsubayashi, H. T., Nihongaki, Y., Flegel, J., Mejdrova, I., Eickhoff, J., Baumann, M., Nencka, R., Janning, P., Kordes, S., Schoeler, H. R., Sterneckert, J., Inoue, T., Ziegler, S., and Waldmann, H. Discovery of the Hedgehog Pathway Inhibitor Pipinib that Targets PI4KIII beta, *Angewandte Chemie-International Edition* **2019**, *58*, 16617-16628.

(32) Llabani, E., Hicklin, R. W., Lee, H. Y., Motika, S. E., Crawford, L. A., Weerapana, E., and Hergenrother, P. J. Diverse compounds from pleuromutilin lead to a thioredoxin inhibitor and inducer of ferroptosis, *Nature Chem.* **2019**, *11*, 521-532.

(33) Paciaroni, N. G., Norwood, V. M., Ratnayake, R., Luesch, H., and Huigens, R. W. Yohimbine as a Starting Point to Access Diverse Natural Product-Like Agents with Re-programmed Activities against Cancer-Relevant GPCR Targets, *Bioorg. Med. Chem.* **2020**, *28*.

(34) Shang, M., Feu, K. S., Vantourout, J. C., Barton, L. M., Osswald, H. L., Kato, N., Gagaring, K., McNamara, C. W., Chen, G., Hu, L., Ni, S. Y., Fernandez-Canelas, P., Chen, M., Merchant, R. R., Qin, T., Schreiber, S. L., Melillo, B., Yu, J. Q., and Baran, P. S. Modular, stereocontrolled C-beta-H/C-alpha-C activation of alkyl carboxylic acids, *Proc. Natl. Acad. Sci. U. S. A.* **2019**, *116*, 8721-8727.

(35) Rentmeister, A., Arnold, F. H., and Fasan, R. Chemo-enzymatic fluorination of unactivated organic compounds, *Nat. Chem. Biol.* **2009**, *5*, 26-28.

(36) Kille, S., Zilly, F. E., Acevedo, J. P., and Reetz, M. T. Regio- and stereoselectivity of P450-catalysed hydroxylation of steroids controlled by laboratory evolution, *Nat. Chem.* **2011**, *3*, 738-743.

(37) Zhang, K. D., Shafer, B. M., Demars, M. D., Stern, H. A., and Fasan, R. Controlled Oxidation of Remote sp(3) C-H Bonds in Artemisinin via P450 Catalysts with Fine-Tuned Regio- and Stereoselectivity, *J. Am. Chem. Soc.* **2012**, *134*, 18695-18704.

(38) Narayan, A. R. H., Jimenez-Oses, G., Liu, P., Negretti, S., Zhao, W. X., Gilbert, M. M., Ramabhadran, R. O., Yang, Y. F., Furan, L. R., Li, Z., Podust, L. M., Montgomery, J.,

Houk, K. N., and Sherman, D. H. Enzymatic hydroxylation of an unactivated methylene C-H bond guided by molecular dynamics simulations, *Nat. Chem.* **2015**, *7*, 653-660.

(39) Zhang, Y., Xiong, Z., Li, Y., Wilson, M., Christensen, K. E., Jaques, E., Hernández-Lladó, P., Robertson, J., and Wong, L. L. Enantioselective oxidation of unactivated C–H bonds in cyclic amines by iterative docking-guided mutagenesis of P450BM3 (CYP102A1), *Nat. Synth.* **2022**, *1*, 936-945.

(40) Kolev, J. N., O'Dwyer, K. M., Jordan, C. T., and Fasan, R. Discovery of potent parthenolide-based antileukemic agents enabled by late-stage P450-mediated C-H functionalization, *ACS Chem. Biol.* **2014**, *9*, 164-173.

(41) Lowell, A. N., DeMars, M. D., Slocum, S. T., Yu, F. A., Anand, K., Chemler, J. A., Korakavi, N., Priessnitz, J. K., Park, S. R., Koch, A. A., Schultz, P. J., and Sherman, D. H. Chemoenzymatic Total Synthesis and Structural Diversification of Tylactone-Based Macrolide Antibiotics through Late-Stage Polyketide Assembly, Tailoring, and C-H Functionalization, *J. Am. Chem. Soc.* **2017**, *139*, 7913-7920.

(42) Alwaseem, H., Giovani, S., Crotti, M., Welle, K., Jordan, C. T., Ghaemmaghami, S., and Fasan, R. Comprehensive Structure-Activity Profiling of Micheliolide and its Targeted Proteome in Leukemia Cells via Probe-Guided Late-Stage C-H Functionalization, *ACS Central Sci.* **2021**, *7*, 841-857.

(43) Le-Huu, P., Rekow, D., Kruger, C., Bokel, A., Heidt, T., Schaubach, S., Claasen, B., Holzel, S., Frey, W., Laschat, S., and Urlacher, V. B. Chemoenzymatic Route to Oxyfunctionalized Cembranoids Facilitated by Substrate and Protein Engineering, *Chem. Eur. J.* **2018**, *24*, 12010-12021.

(44) Loskot, S. A., Romney, D. K., Arnold, F. H., and Stoltz, B. M. Enantioselective Total Synthesis of Nigelladine A via Late-Stage C-H Oxidation Enabled by an Engineered P450 Enzyme, *J. Am. Chem. Soc.* **2017**, *139*, 10196-10199.

(45) Zhang, X., King-Smith, E., Dong, L. B., Yang, L. C., Rudolf, J. D., Shen, B., and Renata, H. Divergent synthesis of complex diterpenes through a hybrid oxidative approach, *Science* **2020**, *369*, 799-+.

(46) Li, J., Li, F. Z., King-Smith, E., and Renata, H. Merging chemoenzymatic and radical-based retrosynthetic logic for rapid and modular synthesis of oxidized meroterpenoids, *Nat. Chem.* **2020**, *12*, 173-+.

(47) Guzman, M. L., Rossi, R. M., Karnischky, L., Li, X., Peterson, D. R., Howard, D. S., and Jordan, C. T. The sesquiterpene lactone parthenolide induces apoptosis of human acute myelogenous leukemia stem and progenitor cells, *Blood* **2005**, *105*, 4163-4169.

(48) Juliana, C., Fernandes-Alnemri, T., Wu, J., Datta, P., Solorzano, L., Yu, J. W., Meng, R., Quong, A. A., Latz, E., Scott, C. P., and Alnemri, E. S. Anti-inflammatory compounds parthenolide and Bay 11-7082 are direct inhibitors of the inflammasome, *J. Biol Chem.* **2010**, *285*, 9792-9802.

(49) Kwok, B. H., Koh, B., Ndubuisi, M. I., Elofsson, M., and Crews, C. M. The anti-inflammatory natural product parthenolide from the medicinal herb Feverfew directly binds to and inhibits IkappaB kinase, *Chem. Biol.* **2001**, *8*, 759-766.

(50) Garcia-Pineres, A. J., Castro, V., Mora, G., Schmidt, T. J., Strunck, E., Pahl, H. L., and Merfort, I. Cysteine 38 in p65/NF-kappaB plays a crucial role in DNA binding inhibition by sesquiterpene lactones, *J. Biol. Chem.* **2001**, *276*, 39713-39720.

(51) Ghantous, A., Gali-Muhtasib, H., Vuorela, H., Saliba, N. A., and Darwiche, N. What made sesquiterpene lactones reach cancer clinical trials?, *Drug Discov. Today* **2010**, *15*, 668-678.

(52) Singh, J., Petter, R. C., Baillie, T. A., and Whitty, A. The resurgence of covalent drugs, *Nat. Rev. Drug Discov.* **2011**, *10*, 307-317.

(53) Boike, L., Henning, N. J., and Nomura, D. K. Advances in covalent drug discovery, *Nat. Rev. Drug Discov.* **2022**, *21*, 881-898.

(54) Zhang, K., El Damaty, S., and Fasan, R. P450 Fingerprinting Method for Rapid Discovery of Terpene Hydroxylating P450 Catalysts with Diversified Regioselectivity, *J. Am. Chem. Soc.* **2011**, *133*, 3242-3245.

(55) Castaneda-Acosta, J., Fischer, N. H., and Vargas, D. Biomimetic transformations of parthenolide, *J. Nat. Prod.* **1993**, *56*, 90-98.

(56) Zhai, J. D., Li, D., Long, J., Zhang, H. L., Lin, J. P., Qiu, C. J., Zhang, Q., and Chen, Y. Biomimetic semisynthesis of arglabin from parthenolide, *J. Org. Chem.* **2012**, *77*, 7103-7107.

(57) Santana, A., Molinillo, J. M. G., and Macias, F. A. Trends in the Synthesis and Functionalization of Guaianolides, *Eur. J. Org. Chem.* **2015**, *2015*, 2093-2110.

(58) Freund, R. R. A., Gobrecht, P., Moser, P., Fischer, D., and Arndt, H. D. Synthesis and biological profiling of parthenolide ether analogs, *Org. Biomol. Chem.* **2019**, *17*, 9703-9707.

(59) Nasim, S., Pei, S., Hagen, F. K., Jordan, C. T., and Crooks, P. A. Melampomagnolide B: a new antileukemic sesquiterpene, *Bioorg. Med. Chem.* **2011**, *19*, 1515-1519.

(60) Burke, M. D., Berger, E. M., and Schreiber, S. L. A synthesis strategy yielding skeletally diverse small molecules combinatorially, *J. Am. Chem. Soc.* **2004**, *126*, 14095-14104.

(61) Galloway, W. R. J. D., Isidro-Llobet, A., and Spring, D. R. Diversity-oriented synthesis as a tool for the discovery of novel biologically active small molecules, *Nat. Commun.* **2010**, *1*.

(62) Zaraei, S. O., Abduelkarem, A. R., Anbar, H. S., Kobeissi, S., Mohammad, M., Ossama, A., and El-Gamal, M. I. Sulfamates in drug design and discovery: Pre-clinical and clinical investigations, *Eur. J. Med. Chem.* **2019**, *179*, 257-271.

(63) Ismail, F. M. D., Levitsky, D. O., and Dembitsky, V. M. Aziridine alkaloids as potential therapeutic agents, *Eur. J. Med. Chem.* **2009**, *44*, 3373-3387.

(64) Carlson, A. S., and Topczewski, J. J. Allylic azides: synthesis, reactivity, and the Winstein rearrangement, *Org. Biomol. Chem.* **2019**, *17*, 4406-4429.

(65) Zhang, T., Gong, T., Yang, Y., Chen, R. Y., and Yu, D. Q. Two new eudesmanolides from Inula racemosa and their bioactivities, *Phytochem. Lett.* **2012**, *5*, 229-232.

(66) Bottcher, T. An Additive Definition of Molecular Complexity, *J. Chem. Inf. Model.* **2016**, *56*, 462-470.

(67) Rogers, D. J., and Tanimoto, T. T. Computer Program for Classifying Plants, *Science* **1960**, *132*, 1115-1118.

(68) Wenderski, T. A., Stratton, C. F., Bauer, R. A., Kopp, F., and Tan, D. S. Principal Component Analysis as a Tool for Library Design: A Case Study Investigating Natural Products, Brand-Name Drugs, Natural Product-Like Libraries, and Drug-Like Libraries, *Methods Mol. Biol.* **2015**, *1263*, 225-242.

(69) Tyagi, V., Alwaseem, H., O'Dwyer, K. M., Ponder, J., Li, Q. Y., Jordan, C. T., and Fasan, R. Chemoenzymatic synthesis and antileukemic activity of novel C9-and C14-functionalized parthenolide analogs, *Bioorgan. Med. Chem.* **2016**, *24*, 3876-3886.

(70) Daina, A., Michielin, O., and Zoete, V. SwissADME: a free web tool to evaluate pharmacokinetics, drug-likeness and medicinal chemistry friendliness of small molecules, *Sci. Rep.* **2017**, *7*.

(71) Roiban, G. D., Agudo, R., Ilie, A., Lonsdale, R., and Reetz, M. T. CH-activating oxidative hydroxylation of 1-tetralones and related compounds with high regio- and stereoselectivity, *Chem. Commun.* **2014**, *50*, 14310-14313.

(72) Lewis, J. C., Mantovani, S. M., Fu, Y., Snow, C. D., Komor, R. S., Wong, C. H., and Arnold, F. H. Combinatorial alanine substitution enables rapid optimization of cytochrome P450BM3 for selective hydroxylation of large substrates, *Chembiochem* **2010**, *11*, 2502-2505.

(73) Ren, X. K., O'Hanlon, J. A., Morris, M., Robertson, J., and Wong, L. L. Synthesis of Imidazolidin-4-ones via a Cytochrome P450-Catalyzed Intramolecular C-H Amination, *ACS Catal.* **2016**, *6*, 6833-6837.

(74) Ren, X. K., Yorke, J. A., Taylor, E., Zhang, T., Zhou, W. H., and Wong, L. L. Drug Oxidation by Cytochrome P450(BM3): Metabolite Synthesis and Discovering New P450 Reaction Types, *Chem.-Eur. J.* **2015**, *21*, 15039-15047.

(75) Venkataraman, H., Beer, S. B., Bergen, L. A., Essen, N., Geerke, D. P., Vermeulen, N. P., and Commandeur, J. N. A single active site mutation inverts stereoselectivity of 16-hydroxylation of testosterone catalyzed by engineered cytochrome P450 BM3, *Chembiochem* **2012**, *13*, 520-523.

(76) van Vugt-Lussenburg, B. M. A., Stjernschantz, E., Lastdrager, J., Oostenbrink, C., Vermeulen, N. P. E., and Commandeur, J. N. M. Identification of critical residues in novel drug metabolizing mutants of cytochrome P450BM3 using random mutagenesis, *J. Med. Chem.* **2007**, *50*, 455-461.

(77) Ren, X. K., and Fasan, R. Engineered and artificial metalloenzymes for selective C-H functionalization, *Curr. Opin. Green Sust.* **2021**, *31*.

(78) Yang, Y., and Arnold, F. H. Navigating the Unnatural Reaction Space: Directed Evolution of Heme Proteins for Selective Carbene and Nitrene Transfer, *Acc. Chem. Res.* **2021**, *54*, 1209-1225.